Proc. of the 9th Intl. Conf. of Asian Society for Precision Engg. and Nanotechnology (ASPEN 2022)
15–18 November 2022, Singapore. Edited by Nai Mui Ling Sharon and A. Senthil Kumar
doi://10.3850/978-981-18-6021-8_OR-07-0020

Some numerical aspects in simulating pad conditioning coverage and density for long time conditioning process

Zhen-Pei Wang#, Zhigang Liu, Zhi-Qian Zhang, Clive S. Ford, N. Sridhar

Institute of High Performance Computing (IHPC), Agency for Science, Technology and Research (A*STAR Research Entities), 1 Fusionopolis Way, 138632, Singapore
Corresponding Author / Email: wangzp@ihpc.a-star.edu.sg, TEL: +65-64191498

KEYWORDS: Pad conditioning, Simulation, Chemical-mechanical polishing/planarization, Error control, Collocation grid method

In a typical chemical-mechanical polishing/planarization process, polishing pads need to be conditioned continuously to ensure appropriate surface characteristics, which significantly affects the pad surface quality. Thus, tuning the conditioning parameters is a crucial step in chip manufacturing to achieve high product quality and reduce manufacturing cost.

The pad conditioning recipe is typically determined with expensive experimental trials. An effective pad conditioning simulation platform to model the conditioning process can significantly reduce the time and cost of the process development cycle. However, to mimic the real-life pad conditioning process, the simulation needs to trace hundreds of conditioning contact points on the conditioner continuously during the conditioning time of many hours. This makes a simulation of pad conditioning, over the whole pad for the duration of the process, very challenging.

In this work, we propose a low-cost numerical approach for simulating the pad conditioning process based on a collocation grid method. Important numerical aspects for simulation efficiency and error control are systematically analyzed and discussed. Some simple benchmark examples are performed to evaluate the effectiveness of the proposed method.

1. Introduction

In semiconductor manufacturing, chemical mechanical planarization (CMP) or polishing is critical to polish IC layers on a silicon wafer to ensure chip quality [1-8]. Typically, the wafer is mounted to a rotating carrier and pressed against a CMP pad affixed on a rotating platen (Fig. 1(a-b)). The CMP pad is made of a soft and porous material that can hold the abrasive grits with the asperities generated by the pad conditioning process. The pad conditioning process, which is essential to maintain the pad surface condition and ensure the CMP quality, is usually achieved using a pad conditioner comprised of diamond tips distributed over a disc (Fig. 1(c)).

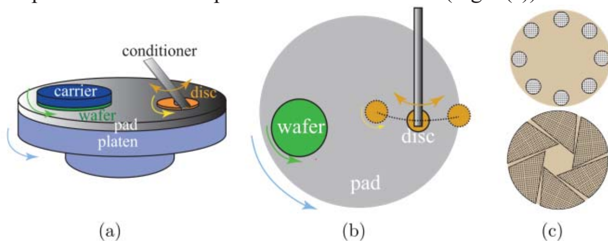

Fig. 1 (a) Major components in a CMP process, (b) kinematics in CMP (top view), and (c) two disc designs with different diamond tip patterns.

In a typical pad conditioning process shown in Fig. 1(b), there are three important motions: pad rotation with a speed of ω_R, the disc rotation with a speed of ω_r, and the sweep motion of the conditioner arm with parameters nested in a vector $\boldsymbol{S}$. The combination of these three motions often leads to a non-uniform pad cutting rate (PCR) along the pad radial direction, which significantly affects the pad surface flatness.

A conditioner consists of a metal disc and diamonds mounted on it. It machines a new pad to create sufficient asperities to hold the grits and restore the asperities by removing the glazing effect during the CMP process. Instead of old designs with randomly distributed diamonds, the latest generation designs of conditioners have a regular distribution of diamonds [9-11], e.g., the designs illustrated in Fig. 1(c), aiming at achieving better control of the conditioning process such that the pad surface can be better maintained, and the pad life can be extended. Diamond distribution on the conditioner also affects the PCR uniformity, which makes it important to design the diamond distribution carefully.

The non-uniformity of the pad surface flatness can lead to severe defections in the pad polishing process. To solve such a problem, a

©2022 ASPEN 2022 Organisers. ISBN: 978-981-18-6021-8. All rights reserved.

detailed conditioning density distribution over the pad needs to be computed such that the output of different conditioning recipes can be evaluated efficiently, which is essential to further tune the conditioning recipes for better outputs [12-16]. However, tracing the trajectory of hundreds of diamond tips over the pad is difficult and costly. In this work, we proposed a collocation grid method with iso-parametric mapping algorithms that essentially reduces the computational cost such that a conditioning density map can be obtained at a low cost.

2. Diamond trajectory tracing

To obtain the pad conditioning density map over the pad, it is necessary to track the trajectories of each diamond feature during a certain processing time period.

Taking the initial pad configuration as the reference frame, the disc center rotates around the pad center at a rotation speed of $-\omega_R$. With no conditioner arm sweep motions, the instantaneous angular location of the disc center on the pad at the time t_i can be computed using

$$\theta_R^{t_i} = -\omega_R t_i + \theta_R^0 + \theta_S^{t_i} \quad (1)$$

in which θ_R^0 represents the initial angular position of the disc center on the pad and $\theta_S^{t_i}$ is the adjustment of the angular position caused by the sweep motions.

The radial coordinate of the disc center on the pad, $L_R^{t_i}$, is determined by the sweep motion. It can be computed together with $\theta_S^{t_i}$, i.e.,

$$[L_R^{t_i}, \theta_S^{t_i}] = f_{sweep}(\boldsymbol{S}, t_i) \quad (2)$$

where $f_{sweep}(\boldsymbol{S}, t_i)$ is a function of the sweep parameters $\boldsymbol{S}$ and time t_i. The $x-$ and y-coordinates of the disc center on the pad can be computed using

$$x_R = L_R^{t_i} \cos(\theta_R^{t_i}) \quad (3)$$

$$y_R = L_R^{t_i} \sin(\theta_R^{t_i}) \quad (4)$$

Taking the initial disc configuration as the reference frame, the angular position of a diamond on the conditioning disc can be evaluated using

$$\theta_r^{t_i} = \omega_r t_i + \theta_r^0, \quad (5)$$

where θ_r^0 represents the initial angular position of the diamond on the disc. Accordingly, the coordinates of the corresponding diamond tip at the disc center can be computed using

$$x_r = L_r^{t_i} cos(\theta_r^{t_i}) \quad (6)$$

$$y_r = L_r^{t_i} sin(\theta_r^{t_i}) \quad (7)$$

where $L_r^{t_i}$ represents the radial coordinates of the diamond tip on the disc.

Eventually, the location of the diamond tip on the pad (i.e., the contact point between the diamond tip and the pad) can be evaluated as $(x_R + x_r, y_R + y_r)$.

At each time step t_i, the relative grid points that have contact with the diamond features are marked and counted into their contact time. With a costly computation, the distribution of the contact time can be computed for each grid point, which is relevant to the cutting depth at different points. This eventually provides a mathematical model to evaluate the outputs (in terms of contact time distribution) of the cutting process with the inputs (in terms of disk moving path, diamond features distribution, etc.).

3. Collocation grid method with parametric mapping space

The framework of the collocation grid method is similar to the reduced-order integration method used in FEM. In this work, the collocation grids are uniformly distributed over the pad, as illustrated in Fig. 2, and each grid, occupying a square region with a side length of l, has a center point located at $\boldsymbol{o} = [x_0, y_0]$. An arbitrary point $\boldsymbol{p} = [x, y]$ is located at the grid region if

$$x_0 - l/2 \le x < x_0 + l/2 \quad (8)$$

$$y_0 - l/2 \le y < y_0 + l/2 \quad (9)$$

and vice versa.

Although using the above criteria is able to determine whether a trajectory point is located at a grid region, finding the region the point belongs to is still a costly process as it requires scanning the grid regions till Eqs.(8-9) are satisfied, which can be very costly if the number of the collocation grids is large.

We propose a parametric space to re-parameterize the pad surface to overcome this problem. Each grid center is located at an integer location, which can be achieved using the following transform function:

$$\boldsymbol{O}^{\mathrm{T}} \coloneqq T(\boldsymbol{o}) = \frac{1}{l}\boldsymbol{I}\boldsymbol{o}^{\mathrm{T}} - \boldsymbol{s}^{\mathrm{T}} \quad (10)$$

where $\boldsymbol{O}^{\mathrm{T}} = [X_0, Y_0]^{\mathrm{T}}$ is the new grid center location in the parametric space with X_0 and Y_0 as integers, $\boldsymbol{I}$ is the identity sensor, and $\boldsymbol{s}^{\mathrm{T}} = [s_x, s_y]^{\mathrm{T}}$ is an offset vector depending on how the periodic grids are placed on the pad. Note that the above transform function is derived based on the relation

$$x_0 = X_0 l + s_x \quad (11)$$

$$y_0 = Y_0 l + s_y \quad (12)$$

and hence the value of X_0 and Y_0 can be guaranteed to be integers.

Henceforth, we can introduce an index function to map each grid region with integer center point locations $[X_0, Y_0]$ to the grid index:

$$I(O) \coloneqq I([X_0, Y_0]) = i, \quad \text{with} \quad i = 1,\ 2,\ \cdots,\ N \quad (13)$$

where N is the total number of the macro collocation grid regions covering the entire pad.

To this end, all the trajectory points are also required to be transformed into the parametric space using \eref{eq:mapFunc}, i.e., for a trajectory point $\boldsymbol{p} = [x, y]^T$ in the physical space, its location in the parametric space is determined as

$$\boldsymbol{P}^{\mathrm{T}} = [X, Y]^{\mathrm{T}} = T(\boldsymbol{p}) = \frac{1}{l}\boldsymbol{I}\boldsymbol{p}^{\mathrm{T}} - \boldsymbol{s}^{\mathrm{T}}. \quad (14)$$

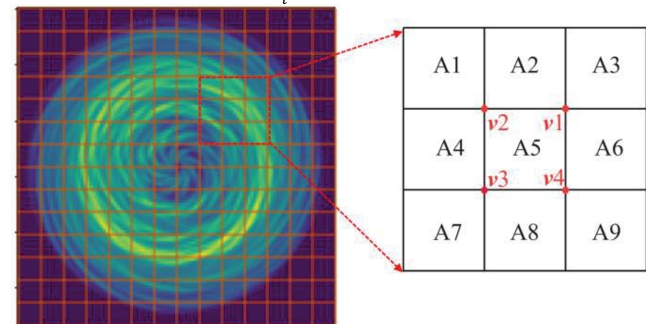

Fig. 2 Schematic of collocation grids over a pad with each grid cell corresponding to an index with integers.

By rounding the value of X and Y to the nearest integer in the parametric space, the grid region where the trajectory point $\boldsymbol{p}$ is

©2022 ASPEN 2022 Organisers. ISBN: 978-981-18-6021-8. All rights reserved.

located can be easily traced using Eq. (13) i.e.,

$$I([[X],[Y]]) = i, \quad \text{with} \quad i = 1, 2, \cdots, N \qquad (15)$$

where $[*]$ is the operator of rounding a number to the nearest integer (with the borderline case 0.5 rounding up according to Eqs.(8-9)). The approach based on the parametric mapping space naturally avoids the complexities of scanning all regions to find where a trajectory point is located, and hence is efficient, regardless of the collocation grid numbers.

4. Time step-size and jump-over ratio

When two neighboring steps locating outside a cell while the path passes the cell, the jump-over trajectories occur, as illustrated in Fig. 3, and the contact over the cell may not be counted. For a grid region with random trajectories, a step-size of δt, and a fixed relative speed v, the sub-regions where the jump-overs may occur are illustrated in Fig. 3(b) with black color, with a total area of $(\delta tv)^2$. Note that the trajectory points can still be located at the black regions, which indicates the chance of jump-overs can be relatively small. Henceforth, the faction of the black regions over the entire region can serve as a relatively conservative upper bound for the jump-over ratio ρ:

$$\rho = \frac{N_\rho}{N_{\text{total}}} = 1 - \frac{N_{\text{rec}}}{N_{\text{total}}} \ll \frac{(\delta tv)^2}{l^2},$$

in which N_ρ is the number of jump-overs of a given cell, N_{rec} is the number of recorded trajectory paths and N_{total} is the total number of all trajectory paths.

This indicates that by choosing a small enough time step-size δt, the jump-over ratio can be reduced to a negligible value. The jump-over ratio may be evaluated using a Monte Carlo method.

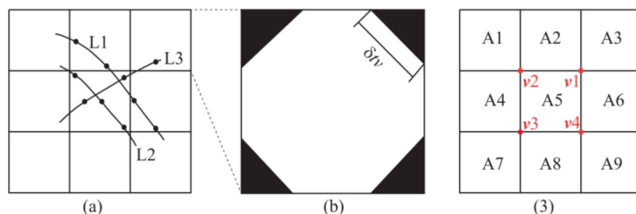

Fig. 3 (a) Illustrations of jump-over trajectories over the center cell (L1) due to a large time step-size is used; (b) Regions where the jump-over issues occur; (c) Index of cells and vertices.

5. Other considerations

The actual implementation also considers

- the evaluation of the best time step-size given the conditioning parameters
- Detailed algorithms for tracking the contact locations and evaluating the jump-over ratio using the Monte Carlo method
- Algorithm to eliminate the repeated counting of the same trajectory over the same cell at adjacent time steps
- Algorithm for total computation time estimation and the full conditioning density map

Due to the length constraint of the manuscript, these details will only not be covered in this manuscript.

6. Results

6.1 Evaluation of the jump-over ratio

Given a unit cell with a size of 1, the jump-over ratios for different δtv are evaluated using a Monte Carlo-based method and the result is plotted in Fig. 4. It shows that by choosing a proper small time step-size, the jump-over ratio can be controlled to a relatively low level, which is beneficial to the overall accuracy of computing the pad conditioning density map.

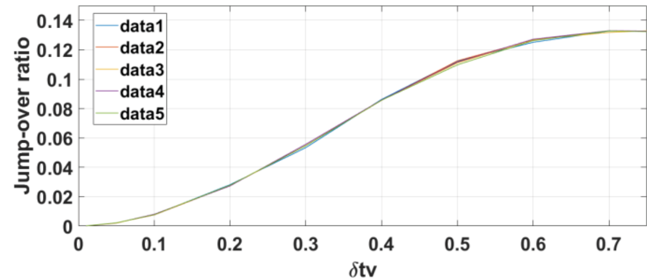

Fig. 4 Jump-over ratio versus the size of δtv for a unit cell with a side length of 1. Big jump-over ratios lead to large errors caused by uncounted trajectories.

6.2 Conditioning simulation

Given a conditioning disc with 6475 diamond tips (Fig. 5(left)), a disc rotation speed of 111rpm, a pad with a radius of 260mm, a pad rotation speed of 90rpm, a mesh grid of 100×100 and a conditioning time of 100 seconds, the simulation time on a ThinkPad P15 with an 11th Generation Intel® Xeon® W-11955M Processor only takes about 2.30 minutes, indicating a high computation efficiency (The result is plotted in Fig. 5(right)).

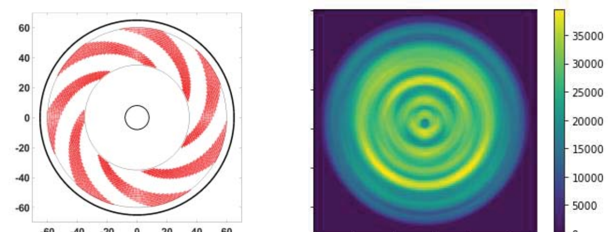

Fig. 5 (left) A conditioning disc with 7 diamond tip blocks, with each block having 925 tips. (right) Conditioning map density over a pad with a radius of 260 mm.

7. Conclusions

This work aims to develop a low-cost numerical approach for simulating long-time pad conditioning process. The approach adopts a collocation grid method with a parametric mapping operation to reduce the cost of tracing the locations of hundreds of diamond feature tips over the pad. Error control of jump-over ratios of trajectory paths over a particular cell is systematically analyzed and discussed. Simple benchmark examples are performed to evaluate the effectiveness of the proposed method.

REFERENCES

1. Borucki, L.J., Witelski, T., Please, C., Kramer, P.R. and Schwendeman, D., 2004. A theory of pad conditioning for

©2022 ASPEN 2022 Organisers. ISBN: 978-981-18-6021-8. All rights reserved.

chemical-mechanical polishing. Journal of Engineering Mathematics, 50(1), pp.1-24.

2. Bastawros, A.-F., Abhijit, C. and Gouda, S. D., 2019. A quantitative analysis of multi-scale response of CMP pad and implication to process assessments. ECS Journal of SolidState Science and Technology 8(5), pp.3145-3153.
3. Park, K.H., Kim, H.J., Chang, O.M. and Jeong, H.D., 2007. Effects of pad properties on material removal in chemical mechanical polishing. Journal of Materials Processing Technology 187, pp.73-76.
4. Fan, W. 2012. Advanced modeling of planarization processes for integrated circuit fabrication. Diss. Massachusetts Institute of Technology.
5. Tsai, C.-H. 2013. Effects of Diamond Disk Dressed Characteristics on the Micro-Scratch Defect of CMP process. Diss. National Chiao Tung University.
6. Oliver, M.R., Robert E.S and Maria R. 2001. CMP pad surface roughness and CMP removal rate. Elec. Soc. S 26, pp.77-83.
7. McGrath, J. and Davis, C., 2004. Polishing pad surface characterisation in chemical mechanical planarisation. Journal of Materials Processing Technology, 153, pp.666-673.
8. Zhao, D. Lu, X., 2013. Chemical mechanical polishing: theory and experiment. Friction, 1, pp.306-326.
9. E. A. Baisie, Z. Li, X. Zhang, Design optimization of diamond disk pad conditioners, The International Journal of Advanced Manufacturing Technology 66 (2013) 2041–2052.
10. M.-Y. Tsai, Polycrystalline diamond shaving conditioner for cmp pad conditioning, Journal of materials processing technology 210 (2010) 1095– 1102.
11. H. Geng, Semiconductor manufacturing handbook, McGraw-Hill Education, 2018.
12. Liu, Z.G., Wan, S., Nguyen, V.B. and Zhang, Y.W., 2014. A numerical study on the effect of particle shape on the erosion of ductile materials. Wear, 313(1-2), pp.135-142.
13. Nguyen, V.B., Nguyen, Q.B., Liu, Z.G., Wan, S., Lim, C.Y.H. and Zhang, Y.W., 2014. A combined numerical–experimental study on the effect of surface evolution on the water–sand multiphase flow characteristics and the material erosion behavior. Wear, 319(1-2), pp.96-109.
14. Baisie, E.A., Li, Z. and Zhang, X., 2013. Pad conditioning in chemical mechanical polishing: a conditioning density distribution model to predict pad surface shape. International Journal of Manufacturing Research, 8(1), pp.103-119.
15. Shin, C., Qin, H., Hong, S., Jeon, S., Kulkarni, A. and Kim, T., 2016. Effect of conditioner load on the polishing pad surface during chemical mechanical planarization process. Journal of Mechanical Science and Technology, 30(12), pp.5659-5665.
16. Li, Z.C., Baisie, E.A. and Zhang, X.H., 2012. Diamond disc pad conditioning in chemical mechanical planarization (CMP): a surface element method to predict pad surface shape. Precision engineering, 36(2), pp.356-363.

©2022 ASPEN 2022 Organisers. ISBN: 978-981-18-6021-8. All rights reserved.